Adsorption of CO on a Platinum (111) surface – a study within a four-component relativistic density functional approach

D. Geschke, T. Baştuğ, T. Jacob, S. Fritzsche, W.-D. Sepp, B. Fricke

Fachbereich Physik, Universität Kassel, D-34109 Kassel, Germany

S. Varga

Department of Experimental Physics,

Chalmers University of Technology, S-41296 Göteborg, Sweden

J. Anton

Department of Atomic Physics, Stockholm University,

Fescativägen 24, S-10405 Stockholm, Sweden

(Dated: January 29, 2002)

Abstract

We report on results of a theoretical study of the adsorption process of a single carbon oxide molecule on a Platinum (111) surface. A four-component relativistic density functional method was applied to account for a proper description of the strong relativistic effects. A limited number of atoms in the framework of a cluster approach is used to describe the surface. Different adsorption sites are investigated. We found that CO is preferably adsorbed at the top position.

PACS: 31.10+z, 31.15.Ew, 31.15.Ne, 31.30.Jv

I. INTRODUCTION

The interaction between atoms and surfaces is essential to understand adsorption processes. In order to determine accurate structures, vibration frequencies, electronic properties and forces *ab initio* calculations are indispensable. Density functional theory (DFT) nowadays provides a powerful tool in nearly all branches of fundamental research in microscopic regimes (see e.g. [1, 2, 3, 4]). It also facilitates a detailed theoretical investigation of problems in surface physics and catalysis on a quantum-chemical level of theory [5], particularly the adsorption process of ad atoms on surfaces within the framework of a molecular orbital picture. Due to the adsorption process on the surface the translation symmetry parallel to the surface is violated. From a strict theoretical point of view methods of solid state physics are no longer applicable for this problem. In order to treat such systems approximately one can use two different approaches; one is the solid state method using super cells or a slab model, and the other is the molecular method using clusters. As the size of the super cell or cluster increases, both methods should converge and yield the correct experimental value. In this paper we follow the molecular approach in which the physical system is approximated by a big molecule or cluster. Results of *ab initio* calculations are comparable with experimental results for small molecular systems and/or clusters. Such a cluster model is of course only an approximation for the description of unlimited surfaces and solids. Nevertheless, as long as the physical process which we are going to describe is strongly localized, a cluster scheme may be an appropriate description. The adsorption process of a single atom or a simple molecule is considered to be such a local effect.

One of the most extensively studied systems in this respect is the adsorption of carbon oxide (CO) on a Platinum surface. However, no good quantitative description has been achieved so far. The reason might be the lack of a proper description of the strong relativistic effects resulting from the $5d$ band of Pt, which lead to a different behaviour in the presence of Pt than on the surfaces of the homologue elements Ni and Pd [6].

We have already tested this cluster approach on simpler systems successfully. The adsorption of a single Na and Ba atom at the Na(110) and the Ba(110) surface, respectively, have been studied [7]. The results were reasonable and encouraged us to apply our method to the more complex system widely used in catalytic processes: the adsorption of CO on a Pt(111) surface.

In this paper we present the results of four-component relativistic density functional calculations for the adsorption of CO on a Pt(111) surface. Recently, our computer code has been developed to a new quality which allows to calculate fragmentation energies and geometries of bigger clusters with local and semi-local density functionals. Compared with scalar relativistic approaches, the spin-orbit coupling is fully included in our formalism.

II. WHAT IS KNOWN FOR THE SYSTEM CO AT PT(111) SO FAR?

The adsorption of CO at a platinum surface seems to be one of the most analyzed experimental systems. Apai et al. [8] showed that the CO molecule is adsorbed linearly with the C bonding towards the surface which can be explained by the fact that the HOMO (5σ) and LUMO ($2\pi^*$) of the CO are located at the C atom. So this site is preferred for a binding with a surface. The molecule does not dissociate after adsorption and the main part of the binding is dominated by the d band of the platinum surface. The CO remains to be effectively neutral.

A theoretical explanation of the binding formalism was given by Blyholder [9]. He studied the binding of CO at metallic surfaces by using a Hückel method. Within this framework the results show a formal charge transfer from the bonding 5σ orbital of the CO towards the metal. On the other hand there is a charge back transfer from the metal towards the anti bonding $2\pi^*$ of the molecule. This exchange of charge explains the fact that the molecule is still neutral after adsorption.

With this theory one is able to distinguish the adsorption site at the surface by the vibrational frequencies of the adsorbed molecule: Effectively there is a charge transfer in the molecule from the bonding 5σ to the anti bonding $2\pi^*$ orbitals. The occupation of the anti bonding orbital leads to a reduced electronic charge between the C and O atom. This results in a weakening of the bonding, and therefore the vibrational frequency of the adsorbed molecule is lowered. The strength of this effect depends on the adsorption site. A molecule adsorbed at a hollow position has a stronger overlap between the metal band and the $2\pi^*$ orbital than at a top position. This is due to the fact that the molecule is closer to the surface. Therefore the frequencies are lower at hollow positions and one is able to distinguish the adsorption sites [9, 10].

Ertl *et al.* [11] reported their results of the adsorption of CO at the Pt(111) surface.

They stated that the strongest bonding arises at a hollow position which they erroneously explained by the knowledge of similar systems like Ni and Pd. With higher coverage the bridge position is occupied building a $\sqrt{(}3) \times \sqrt{(}3)/R30°$ overlay structure. In the regime of zero coverage they estimated the binding energy to be $1.43 \pm 0.04\ eV$. In the following years a lot of experimental papers appeared, discussing the binding energy in this limit of low coverage. The preferred adsorption site is now assumed to be the top position followed by the bridge position [12, 13, 14, 15, 16, 17, 18, 19]. The results show an adsorption energy of 1.3 to 1.6 eV. All these results have one thing in common: The adsorption energy is calculated via the modified Clausius–Clapeyron formula of thermodynamics: Pressure and temperature are varied whereas the coverage is kept constant which is monitored by the change of the work function. The resulting curve is a measure for the adsorption energy. The adsorbed molecules form a dipole layer on the surface resulting in a change of the work function which is proportional to the coverage. In the regime of low coverage this assumption may not be valid.

Newer results of Yeo *et al.* [20] show a significantly stronger binding energy of $1.89 \pm 0.20\ eV$ at low coverage. They used the new Single Crystal Adsorption Calorimetry (SCAC) method which allows the direct measurement of the IR-photon emitted during adsorption.

Somorjai *et al.* were able to estimate the binding distances of the adsorbed molecules. They found a distance of 1.85 ± 0.1 Å between the C atom and the surface at the top position and a value of 1.55 ± 0.07 Å at the bridge position. The bridge position was observed at a coverage of $\frac{1}{3}$. The binding distance within the CO molecule after adsorption is measured to be 1.15 ± 0.05 Å [21, 22]. This is a small elongation of the intra-molecular distance. The free CO molecule has a value of 1.12 Å [23].

On the theoretical side there are a lot of different approaches in the estimation of the binding energy. Most of them use a cluster approach [24, 25, 26, 27, 28, 29, 30, 31, 32, 33] with different methods like modified Hückel methods or pseudopotentials and different numbers of atoms. Some [27, 28, 29, 30] used only 1-2 atoms for the simulation of the surface. The estimated binding energies at the top position are between 0.19 eV and 4.21 eV reflecting the fact that non-relativistic pseudo-potential or Hückel models are not able to give reliable results for the adsorption energy. The main reason for this seems to be the lack of reproducing a good behavior of the d orbitals and therefore the d band of Pt. Models with less than 10 atoms in the cluster will probably only lead by chance to good results. The

Atom Superposition and Electron Delocalization model from Ray and Anderson [25] based on extended Hückel method combined with atomic one particle energies and atom–atom repulsion, on the other hand, leads to acceptable results with a binding energy of 1.66 eV for the top, 1.26 eV for the bridge and 1.11 eV for the *fcc* hollow position followed by 1.03 eV for the *hcp* hollow position. Thus the *fcc* hollow position is slightly preferred among the both possible hollow positions.

Other authors used slab models [34, 35, 36] or a super-cell model [37]. However, all these methods were not applied in the regime of low coverage. They work with an effective coverage between $\frac{1}{4}$ and $\frac{1}{3}$. At these coverages the lateral interactions of the adsorbed molecules are not negligible. Yeo *et al.* [20] showed a decrease of the energy by $0.2 - 0.4\ eV$ within this regime. Thus the results they get are in good agreement with experimental results but are not valid at low coverage.

Brako *et al.* studied the on-top chemisorption of CO molecules as a function of the coverage and the lateral relaxation of the platinum surface using a classical Hamiltonian with an analytical model potential [38].

III. THE THEORETICAL METHOD

We all know that an exact solution of the relativistic many–particle Dirac equation is not possible. Large-scale multi-configuration or coupled cluster approaches are the best approximations for atoms so far. This high quality relativistic calculations are not yet possible for more than diatomic molecules.

For the size of systems we are discussing here only relativistic pseudo-potential or density functional calculations are available. The code which we are using [39] has its first roots in the relativistic version of the DVM approach [40]. Although the general structure of the density functional code has been described in several publications we nevertheless repeat it here in short because a number of details have been modified.

Following the Hohenberg–Kohn [41] and Kohn–Sham theorems [42] and starting from the no-pair approximation [43] and also neglecting the minor important contributions from spatial components of the four-current $j^v(\vec{r}) = (j^0, \vec{j})$, the total energy (in atomic units)

may be written as

$$E[\rho] = T_s + E_N[\rho] + E_H[\rho] + E_{xc}[\rho] \tag{3.1}$$

with the density

$$j^0(\vec{r}) = \rho(\vec{r}) = \sum_{-mc^2 < \varepsilon_k \leq \varepsilon_F} \psi_k^\dagger(\vec{r})\psi_k(\vec{r}) \tag{3.2}$$

obtained from N one-particle Kohn–Sham Dirac spinors. This leads to the corresponding relativistic Kohn-Sham equations [42]

$$\left\{T_s + V^N(\vec{r}) + V^C(\vec{r}) + V^{xc}(\vec{r})\right\}\ \psi_i(\vec{r}) \ = \ \epsilon_i\,\psi_i(\vec{r}). \tag{3.3}$$

Here $T_s = c\,\alpha_i\,p_i + (\beta - 1)c^2$ is the relativistic operator of the electronic kinetic energy, $V^N(\vec{r})$ represents the nuclear potential assumed as a sum of point charges

$$V^N(\vec{r}) = \sum_\nu \frac{Z_\nu e^2}{\vec{R}_\nu - \vec{r}}\ , \tag{3.4}$$

$V^{xc}(\vec{r})$ is the exchange–correlation potential derived from the exchange–correlation energy E_{xc}

$$V^{xc}(\vec{r}) = \frac{\delta\,E_{xc}[\rho]}{\delta\rho(\vec{r})}\ \ . \tag{3.5}$$

For the self-consistent solution of equation (3.3) we use the relativistic local density approximation [44, 45] (RLDA) together with the Vosko, Wilk and Nusair parameterization [46] for correlation. Nonlocal corrections, with the relativistic form (RGGA) [47] of Becke's GGA approximation[48] for exchange and Perdew functional of correlation [49] (B88/P86)is used perturbatively. Optionally we also have a relativistic extension of Perdew and Wang [50] (PW91) for the xc-energy. The Coulomb potential $V^C(\vec{r})$ is given by

$$V^C(\vec{r}) = \int \frac{\rho(\vec{r'})}{|\vec{r} - \vec{r'}|}\,d^3r'. \tag{3.6}$$

Numerical evaluation of the Coulomb matrix elements requires the evaluation of the Coulomb potential at the grid points, which leads to a large number (n^2p; n: number of basis functions, p: number of grid points) of nuclear attraction type integrals. It is possible to facilitate the n^2p problem by approximating the exact density with an expansion in one center fit functions

$$\widetilde{\rho}(\vec{r}) \ = \ \sum_{\alpha=1}^{A} \sum_{r=1}^{M_\alpha} \sum_{l=0}^{L_r} \sum_{m=-l}^{l} d_{rm}^{\alpha\,l}\, f_\alpha^r(\chi_\alpha)\, Y_l^m(\theta_\alpha, \phi_\alpha), \tag{3.7}$$

where $f_\alpha^r(\chi_\alpha)$ is the radial density of the wave function r of atom α. χ_α is a radial vector centered at each atom $\vec{\chi_\alpha} = \vec{r} - \vec{R}_\alpha$. $d_{rm}^{\alpha l}$ are the expansion coefficients of the approximate density which are obtained via a least square fit to the density (3.2)

$$\int (\rho(\vec{r}) - \widetilde{\rho}(\vec{r}))^2 \, d^3r \quad , \tag{3.8}$$

or via minimizing the Coulomb energy of the difference density [51]

$$\int \frac{(\rho(\vec{r}) - \widetilde{\rho}(\vec{r}))(\rho(\vec{r}) - \widetilde{\rho}(\vec{r}))}{|\vec{r} - \vec{r'}|} \, d^3r' d^3r \quad . \tag{3.9}$$

For simpler molecules, that means without complex density structure, it was sufficient to use only the monopole part of the atomic wave functions to build the approximate density. With the open d shell of Pt it is necessary to use higher moments in the expansion (3.7). Actually we use values up to $l = 2$. Using this procedure the least square value of eqn. (3.8) was less than 5%.

With the use of the approximate density (3.7) we can reduce the three dimensional integral in equation (3.6) to one dimensional integrals:

$$V(\vec{r}) \;=\; \sum_{\alpha}^{A} \sum_{r=1}^{M_\alpha} \sum_{l=0}^{L_r} \sum_{m=-l}^{l} d_{rm}^{\alpha l} \, V_{\alpha l}^{rm}(\chi_\alpha)$$

with

$$V_{\alpha l}^{rm}(\chi_\alpha) \;=\; \frac{4\,\pi}{2\,l+1} \frac{1}{\xi_\alpha^{l+1}} Y_l^m(\theta_\alpha, \phi_\alpha) \left[\int_0^{\chi_\alpha} \xi_\alpha'^{\,l+2} \, f_\alpha^r(\xi_\alpha') d\xi_\alpha' + \xi_\alpha^{2\,l+1} \int_{\chi_\alpha}^{\infty} \frac{1}{\xi_\alpha'^{\,l-1}} \, f_\alpha^r(\xi_\alpha') d\xi_\alpha' \right] .$$

In order to solve the Kohn-Sham equations (3.3) we use the Molecular-Orbital Linear Combination of Atomic Orbitals (MO-LCAO)-method and expand the molecular orbital wave functions in symmetry–adapted wave function χ_j, which themselves are expanded in atomic orbitals $\chi_{n_\nu}(\vec{r})$ which are atomic four–component Dirac–Spinors[52, 53]

$$\psi_i(\vec{r}) \;=\; \sum_j \chi_j(\vec{r}) c_{ji} \tag{3.10}$$

$$\chi_j(\vec{r}) \;=\; \sum_{n_\nu} \chi_{n_\nu}(\vec{r}) d_{n_\nu j} \tag{3.11}$$

with $n_\nu = (\nu, n, \kappa, m)$. Here $\chi_{n_\nu}(\vec{r})$ are the relativistic four–component atomic basis functions centered at the atoms. Using this symmetry adapted atomic basis set implies the non pair approximation [43]. The symmetry coefficients $d_{n_\nu j}$ are calculated by the program

TSYM of Meyer [52, 53]. The expansion coefficients c_{ij} of the molecular wave functions together with the one-particle energies ϵ_i are the results of the SCF calculation of equation (3.3). Inserting (3.10) into (3.3) gives the matrix secular equation in the symmetry orbital basis χ,

$$\mathbf{HC} = \varepsilon\mathbf{SC} \tag{3.12}$$

where **H** and **S** are the Hamiltonian and overlap matrices respectively, **C** is the coefficient-matrix (c_{ij}) and ε is the eigenvalue-vector (ε_i). The matrix elements, H_{ij} and S_{ij} are evaluated numerically using the multi-center integration scheme by Baerends et al. [54, 55]. In this scheme the whole molecular volume is spatially partitioned into so called Voronoi cells and each cell is divided into an atomic sphere around the atomic nucleus and polyhedra. This method was extended by a special transformation to account for the relativistic behavior of the wave function near the nuclei [39].

IV. THE FROZEN–CORE APPROXIMATION

In order to reduce the computational requirement one very popular way is to use either pseudopotentials or the Frozen Core approximation (FCA). Both approximations are based on the idea that chemical binding is realized via the outer valence orbitals only. In our calculations we used the Frozen Core Approximation. In FCA it is assumed that the inner orbitals do not change their form during the adsorption process so that they can be kept fixed in the self consistence procedure. This reduces the numerical effort for the heavier elements like Pt drastically.

Since the FCA is a very popular approximation and used in almost all kinds of *ab initio* calculations (from density functional to quantum chemical methods) there are many references in the literature [56, 57, 58] for this method.

Although the principal procedure of the FCA in all *ab initio* methods is the same, there are differences in practical implementations. Therefore we give a short summary of the FCA in our code. Compared with all electron calculations there are two differences in FC calculations: the orthogonalization of the valence orbitals to the core orbitals and the calculation of the total energy.

The FCA is based on a decomposition of the Hilbert space into a core (c) and a valence

(v) part. Accordingly, the molecular wave functions can be written as:

$$|\psi\rangle = |\psi_v\rangle + |\psi_c\rangle.$$

In order to ensure the constrained Ritz variation of the valence orbitals, a core-valence orthogonalization has to be carried out. In our implementation we followed the idea of the normalization of the overlap matrix in the core-valence orthogonalization. The decomposition of the Hilbert space results in the decomposition of the overlap and Fock matrices into core-core, core-valence and valence-valence parts which have to be orthogonalized to each other.

In order to ensure the core-valence orthogonalization all contributions of core orbitals are removed from the valence orbitals. This is achieved by the explicit orthogonalization of the valence orbitals onto the core orbitals.

$$|\chi'_v\rangle \;=\; |\chi_v\rangle - S_{vc}\, S_{cc}^{-1}\, |\chi_c\rangle.$$

Here S_{vc} is the valence–core overlap matrix. As a result the transformed overlap and Fock matrices of the whole system are now of the form:

$$\mathrm{S'} = \begin{pmatrix} S_{cc} & 0 \\ 0 & S'_{vv} \end{pmatrix} \quad ; \quad \underline{\underline{\mathrm{H}}} = \begin{pmatrix} H_{cc} & 0 \\ 0 & H'_{vv} \end{pmatrix} + \underbrace{\begin{pmatrix} 0 & H'_{vc} \\ H'_{cv} & 0 \end{pmatrix}}_{\rightarrow neglected}. \tag{4.1}$$

We assume that the core orbitals of different atoms do not overlap. By the use of atomic orbitals the core orbitals of the same atom are by default orthogonal. Therefore the corresponding symmetry orbitals are also orthonormal and $S_{cc} = 1$.

Due to the chemical binding the relative change in the core potential is small. The change in the core wave functions which is a second order effect can therefore be neglected. This means that H'_{vc} in eqn. (4.1) can be neglected. As a result of this approximation the secular equation (3.12) decouples into two equations, which are solved like all electron calculations. Both approximations define our implementation of FCA.

The total energy within this Frozen–Core approximation is now:

$$
\begin{aligned}
E \;=\; & \sum_{\alpha=1}^{A} \sum_{\mu=1}^{N_\alpha^c} n_{\alpha\mu}^{c}\, \epsilon_{\mu}^{\alpha} - \frac{1}{2} \sum_{\alpha=1}^{A} \int v_{c\alpha}^{C}\, \rho_c^{\alpha}\, d^3r \\
& - \sum_{\alpha=1}^{A} \int v_{v\alpha}^{C}\, \rho_c^{\alpha}\, d^3r - \sum_{\alpha=1}^{A} \int v_{\alpha}^{xc}\, \rho_c^{\alpha}\, d^3r \\
& + \sum_{\alpha=1}^{A} \sum_{\beta\neq\alpha}^{A} \int v_{\alpha}^{N}\, \rho_c^{\beta}\, d^3r + \frac{1}{2} \sum_{\alpha=1}^{A} \sum_{\beta\neq\alpha}^{A} \int v_{c\alpha}^{C}\, \rho_c^{\beta}\, d^3r \\
& + \sum_{i=M^c+1}^{M} n_i^v\, \epsilon_i - \frac{1}{2} \int \widetilde{\rho}^{v}\, \widetilde{V}_v^{C}\, d^3r - \int V^{xc} \rho_v\, d^3r \\
& + E^{xc} + \sum_{\substack{\alpha,\beta=1 \\ \alpha<\beta}}^{A} \frac{Z_\alpha\, Z_\beta}{|\vec{R}_\alpha - \vec{R}_\beta|}.
\end{aligned}
\tag{4.2}
$$

The symbols with a small v represent atomic potentials. The subindices c and v mean that the core and valence densities are used to calculate the potentials. The first two lines of equation (4.2) consist of pure atomic contributions. As far as we do not change the basis functions these values can be neglected as long as we are only interested in binding energies and distances. In this case these core contributions cancel completely out. The third line describes only the core–core interactions of different atoms. These values can be approximated by the use of point charges:

$$
\begin{aligned}
\sum_{\substack{\alpha,\beta=1 \\ \beta\neq\alpha}}^{A} \int v_{\alpha}^{N}\, \rho_c^{\beta}\, d^3r + \frac{1}{2} \sum_{\substack{\alpha,\beta=1 \\ \beta\neq\alpha}}^{A} \int v_{c\alpha}^{C}\, \rho_c^{\beta}\, d^3r \;&=\; \sum_{\alpha=1}^{A} \sum_{\beta\neq\alpha}^{A} \int \rho_c^{\beta}\, (v_{\alpha}^{N} + v_{c\alpha}^{C})\, d^3r \\
&\approx\; - \sum_{\alpha=1}^{A} \sum_{\beta\neq\alpha}^{A} \frac{Z_\beta^c\, (Z_\alpha - \frac{1}{2} Z_\alpha^c)}{|\vec{R}_\alpha - \vec{R}_\beta|}.
\end{aligned}
$$

The last two lines are exactly the same as in the total energy expression in an all electron calculation but only with the use of the new valence orbitals for the density. For V^{xc} we still need the full density $\rho = \rho_c + \rho_v$.

V. RESULTS

Our aim in this paper is the *ab initio* calculation of the adsorption of CO at Pt(111) surface. This process is one of the most frequently used catalytic processes but is not

understood in detail up to now. We have referred to the experimental findings and theoretical methods which were applied up to now in section II.

As Pt is a very heavy metal where relativistic effects play an important role we at least have the appropriate method. Unfortunately the computational effort restricts the actual calculations to a very limited number of Pt atoms which can be used in a real calculation. Nevertheless we have achieved to converge clusters between 7 and 13 Pt atoms depending on the adsorption site of the CO molecule. To keep the calculation time in an acceptable range, we in addition used only a quasi minimal basis set which was optimized via the degree of ionization of the atomic wave functions used as basis functions. For Pt we use the $1s$ to $6p$ wave functions with a degree of ionization of $+0.2$. As an effect this leads to valence functions which are slightly more localized than the neutral ones but are more suitable to reproduce the binding character of the bulk. For the wave functions with the main quantum numbers n=1 to 4 in addition the FCA was used.

A. The CO molecule

For the calculation of the CO molecule a larger basis set was used. This system requires a very good basis to account for the strong chemical bonding and charge distribution within this molecule.

The best results for the CO molecule were obtained with a minimal basis set consisting of the $1s - 2p$ wave functions of the neutral atoms in combination with additional $3p, 3d$ wave functions with an degree of ionization of $+4.0$. In this molecule all electrons were used in the SCF process.

Table I shows the results for the CO molecule, which are close to the experimental data. The negative value of the dipole moment indicates a major negative charge at the C atom. The binding energy is slightly too high, which may be attributed to an unpolarized treatment because current-dependent functionals are not available.

B. The adsorption calculations

In order to calculate the adsorption energy of CO on the Pt(111) surface one first has to define the clusters which simulate the surface for the four possible adsorption sites of

the CO molecule. The internuclear axis of the CO molecule is assumed to be perpendicular to the surface with C towards the surface. The four possible adsorption sites are the top, bridge, fcc–hollow and hcp–hollow of the (111) surface of Pt. The different adsorption sites are shown in Figures 1 to 4. As insert in the figures 1 to 4 we present the Pt–clusters as molecular models in the view from above and in a perspective view for the four adsorption sites. The CO molecule can also be seen. The distances between the Pt atoms are kept fixed to their bulk values ($a_0 = 3.92$ Å) and the CO distance to the value calculated above.

In the cases of top and the hollow positions the C_{3v} symmetry was utilized. For the bridge position only a C_{1h} symmetry can be used. Figures 1 to 4 show the results of the calculations. Because of the low symmetry of the bridge position a maximum of 7 atoms had to be used to get results in a realistic calculation time. The notation $\mathrm{Pt}_{m+n}(m,n)$ denotes the number of atoms per layer: m atoms in the first layer and n in the second resulting in $m+n$ total Pt atoms. The bulk was represented only by two layers. As shown in the literature, this number of layers seems to be necessary and nearly sufficient [60, 61, 62].

Results of our calculations for binding of the CO molecule on the four surfaces are given in Tables II–IV for the GGA calculations according to Becke 1988 [48] in combination with Perdew 1986 [49] (which in short term notation is B88/P86).

The results show the experimentally observed binding order with the top position as the strongest one and therefore as the preferred adsorption site. Like Ray and Anderson [25] we also find a slight preference of the fcc position in the hollow positions.

Within our method the binding energies are by about $10-20\%$ too high compared with experimental results (see for instance the results of the CO molecule). Having this in mind our results of 2.3 eV binding energy at the top position compares well with the measured value of 1.86 ± 0.20 eV of Yeo *et al.* [20] (see table II). A direct comparison of binding energies at other positions with experimental results is not available. The calculations here were performed with a single CO molecule only. In experiments an occupation of the other adsorption sites is only observed at much higher coverages which are not considered here.

In Table III the calculated bond distances of the C atom (of the CO molecule) with respect to the surface at the energy minimum at the four possible adsorption sites are listed.

In addition very informative is Table IV. Here the distances are calculated towards the next Pt atom of the surface for all four CO positions. For better comparison with the experimental results these values are converted to Å. These results correlate with the binding

behaviour. The distance at top position is the shortest whereas the hollow positions have the greatest distances. A comparison with the experimental values shows a good agreement for the top position as well as the bridge position where our value is slightly shorter than the experimental value. One reason for this may lie in the effective coverage when the bridge position is experimentally observed. As already mentioned, the interactions of the adsorbed CO molecules are not negligible [24] within this coverage.

Table V presents a comparison of our values for the top–position with other theoretical results. These values demonstrate that the bond energies still do scatter up to 1 eV. The same applies for the various theoretical results for the hollow–position in Table VI.

Table VII shows the electronic charge distribution of the CO molecule as a result of a Mulliken population analysis of our calculations. The charge of the oxygen atom remains more or less constant and independent of the adsorption process and adsorption site whereas the carbon atom changes its charge by small amounts. A more detailed analysis of the electronic charge distribution shows that the charge between the two atoms C and O is reduced in the direction off the molecular axis.

It is further interesting to see that the CO molecule as a whole has almost no charge transfer at the top position which has the strongest binding whereas all three other positions show a negative charge transfer from the cluster to the molecule of nearly half an electron.

In addition we studied the effect of elongation of the CO distance on the top–position adsorption site. As a result we found only a very small elongation of $0.01-0.02$ $a.u.$ compared with the free molecule.

VI. CONCLUSION

Using a cluster approach within a relativistic density functional approximation as described above, we get results for the adsorption of the CO molecule on the Pt(111) surface which are reasonably good. This statement in itself is very remarkable although we must admit that we are not able to show the convergence of these results with cluster size here. For one of the positions we have been able to include more Pt atoms in the cluster and in fact, the binding energy did not change any more. As expected, the binding energy is slightly higher than the experimental value of Yeo *et al.* [20].

Finally we note that the used method is able to describe the adsorption process. We are

able to calculate this important system with a quasi *ab initio* method (the only experimental result used in the calculation is the structure of the bulk) in a fully relativistic framework. In our calculations all relativistic d orbitals of Pt are treated dynamically.

VII. ACKNOWLEDGMENT

T.B. gratefully acknowledges support from the Alexander von Humboldt Foundation (AvH), T.J. from the Studienstiftung des Deutschen Volkes, S.V. from the German Academic Exchange Service (DAAD) and J.A. from the Deutsche Forschungsgemeinschaft.

---

[1] T. M. Alam, *Biophys. J.* **64**, 1681 (1993)

[2] D. Boda, D. Henderson, R. Rowley, S. Sokolowsky, *J. Chem. Phys* **111**, 9382 (1999)

[3] S. K. Nath, P. F. Nealey, J. J. de Pablo, *J. Chem. Phys* **110**, 7483 (1999)

[4] C. N. Patra and A. Yethiraj, *J. Chem. Phys* **112**, 1579 (2000)

[5] C. R. Henry, *Surf. Sci. Rep.* **31**, 232 (1998)

[6] G. Pacchioni, S. Chung, S. Krüger, N. Rösch, *Surf. Sci.* **392**, 173 (1997)

[7] D. Geschke, S. Fritzsche, W.-D. Sepp, B. Fricke, S. Varga, J. Anton, *Phys. Rev. B* **62**, 15439 (2000)

[8] G. Apai, P. S. Wehner, R. S. Williams, J. Stöhr, D. A. Shirley,*Phys. Rev. Lett.* **37**, 1497 (1976)

[9] G. Blyholder, *J. Phys. Chem.* **68**, 2772 (1964)

[10] G. Ganteför, G. Schulze Icking–Konert, H. Handschuh, W. Eberhardt, *International Journal of Mass Scpetrometry and Ion Processes* **159**, 81 (1996)

[11] G. Ertl, M. Neumann, K. M. Streit, *Surface Science* **64**, 393 (1977)

[12] H. Froitzheim, H. Hopster, H. Ibach, S. Lehwald, *Applied Physics* **13**, 147 (1977)

[13] R. W. McCabe, L. D. Schmidt, *Surface Science* **65**, 189 (1977)

[14] H. Horn, J. Pritchard, *J. Physique* **38**, 147 (1977)

[15] H. Hopster, H. Ibach, *Surface Science* **77**, 109 (1978)

[16] S. R. Kelemen, T. E. Fischer, J. A. Schwarz, *Surface Science* **81**, 440 (1979)

[17] D. H. Winicur, J. Hurst, C. A. Becker, L. Wharton, *Surface Science* **109**, 263 (1981)

[18] H. Steiniger, S. Lehwald, H. Ibach, *Surface Science* **123**, 164 (1982)

[19] E. G. Seebauer, A. C. F. Kong, L. D. Schmidt, *Surface Science* **176**, 134 (1986)

[20] Y. Y. Yeo, L. Vattuone, D. A. King, *J. Chem. Phys.* **106**, 392 (1997)

[21] D. F. Ogletree, M. A. Van Hove, G. A. Somorjai, *Surface Science* **173**, 351 (1986)

[22] G. S Blackman, M.-L. Xu, D. F. Ogletree, M. A. Van Hove, G. A. Somorjai, *Phys. Rev. Lett.* **61**, 2352 (1988)

[23] K. P. Huber, G. Herzberg, *Molecular Spectra and Molecular Structure: IV. Constants of Diatomic Molecules*, Van Nostrand Reinhold Company, New York (1979)

[24] D. R. Jennison, P. A. Schultz, M. P. Sears, *Phys. Rev. Lett.* **77**, 4828 (1996)

[25] N. Ray, A. B. Anderson, *Surface Science* **119**, 35 (1982)

[26] A. Gavezzotti, G. F. Tantardini, H. Miessner, *J. Phys. Chem.* **92**, 872 (1988)

[27] Y.-T. Wong, R. Hoffmann, *J. Phys. Chem.* **95**, 859 (1991)

[28] S. Roszak, K. Balasubramanian, *Chem. Phys. Lett.* **212**, 150 (1993)

[29] S. Roszak, K. Balasubramanian, *J. Phys. Chem.* **97**, 11238 (1993)

[30] S. Roszak, K. Balasubramanian, *J. Chem. Phys.* **103**, 1043 (1995)

[31] S. Ohnishi, N. Watari, *Phys. Rev. B* **49**, 14619 (1994)

[32] F. Illas, S. Zurita, A. M. Márquez, J. Rubio, *Phys. Rev. B* **52**, 12372 (1995)

[33] F. Illas, S. Zurita, J. Rubio, A. M. Márquez, *Surface Science* **376**, 279 (1997)

[34] B. Hammer, Y. Morikawa, J. K. Nørskov, *Phys. Rev. Lett.* **76**, 2141 (1996)

[35] P. H. T. Philipsen, E. van Lenthe, J. G. Snijders, E. J. Baerends, *Phys. Rev. B* **56**, 13556 (1997)

[36] Anton Kopalj, M. Causà *J. Phys.: Condens. Matter* **11**, 7463 (1999)

[37] Y. Morikawa, J. J, Mortensen, B. Hammer, J. K. Nørskov, *Surface Science* **386**, 67 (1997)

[38] R. Brako, D. Šokčević, *Surf. Sci.* **401**, L388 (1998)

[39] T. Baştuğ, W.-D. Sepp, D. Kolb, B. Fricke, G. te Velde, E. J. Baerends, *J. Phys. B:At. Mol. Opt. Phys.* **28**, 2325–2331 (1995)

[40] A. Rosén, D. E. Ellis *J. Chem. Phys.* **62**, 3030 (1975)

[41] P. Hohenberg, W. Kohn, *Phys. Rev. B* **136**, 864 (1964)

[42] W. Kohn, L. J. Sham, *Phys. Rev. A* **140**, 1133 (1965)

[43] W.–D- Sepp and B. Fricke, *AIP Conf. Proc.* **136**, 20 (1986)

[44] A. K. Rajagopal, *J. Phys. C* **11**, L943 (1978)

[45] A. K. Rajagopal, J. Callaway, *Phys. Rev. B* **7**, 1912 (1973)

[46] S. H. Vosko, L. Wilk, M. Nusair, *Can. J. Phys.* **58**, 1200 (1994)

[47] E.Engel, S.Keller, R.M.Dreizler, *Phys. Rev.* **A53**, 1367 (1996)

[48] A. D. Becke, *Phys. Rev. A* **38**, 3098 (1988)

[49] J. P. Perdew, *Phys. Rev. B* **22**, 8822 (1986)

[50] *Electronic Structure of Solids 1991*, ed. P. Ziesche, H. Eschrig, Akademieverlag, Berlin (1991)

[51] T. Baştuğ, D. Heinemann, W.-D. Sepp, D. Kolb, and B. Fricke, *Chem. Phys. Lett.* **211**, 119–124 (1993)

[52] J. Meyer, W.-D. Sepp, B. Fricke, and A. Rosén, *Int. J. Quantum Chem.* **33**, 445 (1988)

[53] J. Meyer, W.-D. Sepp, B. Fricke, and A. Rosén, *Int. J. Quantum Chem.* **61**, 929 (1997)

[54] P. M. Boerrigter, G. te Velde, E. J. Baerends, *Int. J. Quant. Chem* **33**, 87 (1988)

[55] G. te Velde, E. J. Baerends, *J. Computational Phys.* **99**, 84 (1992)

[56] W. H. Fink, *J. Chem. Phys.* **57**, 1822 (1972)

[57] J. Hinze, *Adv. Chem. Phys.* **26**, 213 (1974)

[58] Y. Watanabe, O. Matsuoka, *J. Chem. Phys.* **109**, 8182 (1998)

[59] J. S. Muenter, *J. Mol. Spectrosc.* **55**, 490 (1975)

[60] G. Wiesenekker, H. J. Kroes, E. J. Baerends, R. C. Mowrey, *J. Chem. Phys.* **102**, 3873 (1995)

[61] P. H. T. Philipsen, G. te Velde, E. J. Baerends, *Chem. Phys. Lett.* **226**, 583 (1994)

[62] V. Castells, O. Atabek, A. Beswick, *J. Chem. Phys.* **110**, 4907 (1999)

Table Capture

Table I. Results for the CO molecule: binding energy (BE), binding distance (d_{C-O}), ionisation potential (IP), frequency (ω_{C-O}) of the molecular stretch vibration and dipole moment (μ). The dipole moment was calculated at the distance of the energy minimum. Assuming the experimental binding distance a value of $\mu = -0.052$ a.u. was obtained.

Table II. Results for the binding energy of CO on Pt(111) in eV for the four adsorption sites.

Table III. Results for the distance of the carbon atom to the surface (in a.u.) for the four bond positions.

Table IV. Comparison of the results of the distance of the carbon atom to the next surface platinum atom (in a.u.).

Table V. Comparison of theoretical results for the top–position.

Table VI. Comparison of theoretical results for the hollow–position.

Table VII. Electronic charge of the adsorbed molecule and the consisting atoms as a result of a Mulliken population analysis for CO at Pt(111).

Funktional	RLDA	B88/P86	Experiment
BE (eV)	14.18	13.25	11.09 [23]
d_{C-O} (Å)	1.148	1.153	1.128 [23]
IP (eV)	15.01	15.11	14.01 [23]
$\omega_{C-O}(cm^{-1})$	2281.11	2176.22	2169.81 [23]
μ (a.u.)	-0.027	-0.020	-0.046 [59]

TABLE I:

Figure Capture

Figure 1. Potential energy curve of CO on Pt(111) at the top position. The platinum cluster consists of 13 atoms: $Pt_{13}(7,6)$. Solid curve is obtained with B88 exchange and BP86 correlation potential and dotted curve is obtained with PW91 exchange and correlation potential.

Figure 2. Potential energy curve of CO on Pt(111) at the bridge position. The platinum cluster onsists of 7 atoms: $Pt_7(4,3)$. Solid curve is obtained with B88 exchange and BP86 correlation potential and dotted curve is obtained with PW91 exchange and correlation potential.

Figure 3. Potential energy curve of CO on Pt(111) at the *fcc* hollow position. The Platinum cluster consists of 12 atoms: $Pt_{12}(6,6)$. Solid curve is obtained with B88 exchange and BP86 correlation potential and dotted curve is obtained with PW91 exchange and correlation potential.

Figure 4. Potential energy curve of CO on Pt(111) at the *hcp* hollow position. The platinum cluster consists of 13 atoms: $Pt_{13}(6,7)$. Solid curve is obtained with B88 exchange and BP86 correlation potential and dotted curve is obtained with PW91 exchange and correlation potential.

Energy functional	top-position	bridge-position	*hcp* hollow-position	*fcc* hollow-position
RLDA	3.25	3.15	3.35	3.25
B88/P86	**2.30**	**1.87**	**1.65**	**1.76**
Experiment [20]	1.86 ± 0.20	—	—	—

TABLE II:

Energy functional	top-position	bridge-position	*hcp* hollow-position	*fcc* hollow-position
RLDA	3.50	2.60	2.55	2.55
B88/P86	**3.57**	**2.70**	**2.65**	**2.65**

TABLE III:

Energy functional	top-position	bridge-position	*hcp* hollow-position	*fcc* hollow-position
RLDA	3.50	3.69	3.95	3.95
B88/P86	**3.57**	**3.76**	**4.03**	**4.03**
Experiment [21, 22]	3.50 ± 0.19	3.93 ± 0.13	—	—

TABLE IV:

method	$r_{Pt-C}[a.u.]$	E_b(eV)	Ref.	Explanation
RLDA	3.50	3.25	this work	13 Pt atoms, 2 layers (7,6)
RGGA	3.57	2.30	this work	13 Pt atoms, 2 layers (7,6)
CASSCF	3.84	1.44	[30]	Complete Active Space
PP-Slab	3.55	1.45	[34]	6 layers slab
ZORA-DFT GGA	3.59	1.41	[35]	spin-orbit, 2 layers slab
exp.	3.49 ± 0.19		[21, 22]	

TABLE V:

method	$r_{Pt-C}[a.u.]$	E_b(eV)	Ref.	Explanation
RLDA	3.95	3.25	this work	9 Pt atoms; 2 layers (6,3)
RGGA	4.02	1.76	this work	9 Pt atoms; 2 layers (6,3)
ORPP	3.96	2.39	[26]	optimized relativistic pseudo potential
ZORA-DFT GGA	4.12	1.05	[35]	pin-orbit, 2 layers slab
exp.	3.93 ± 0.13		[21, 22]	

TABLE VI:

	top-position	bridge-position	*hcp* hollow-position	*fcc* hollow-position	free molecule
Oxygen	8.375	8.370	8.359	8.359	8.348
Carbon	5.719	6.072	6.094	6.075	5.652
Sum	14.094	14.442	14.453	14.434	14.000

TABLE VII:

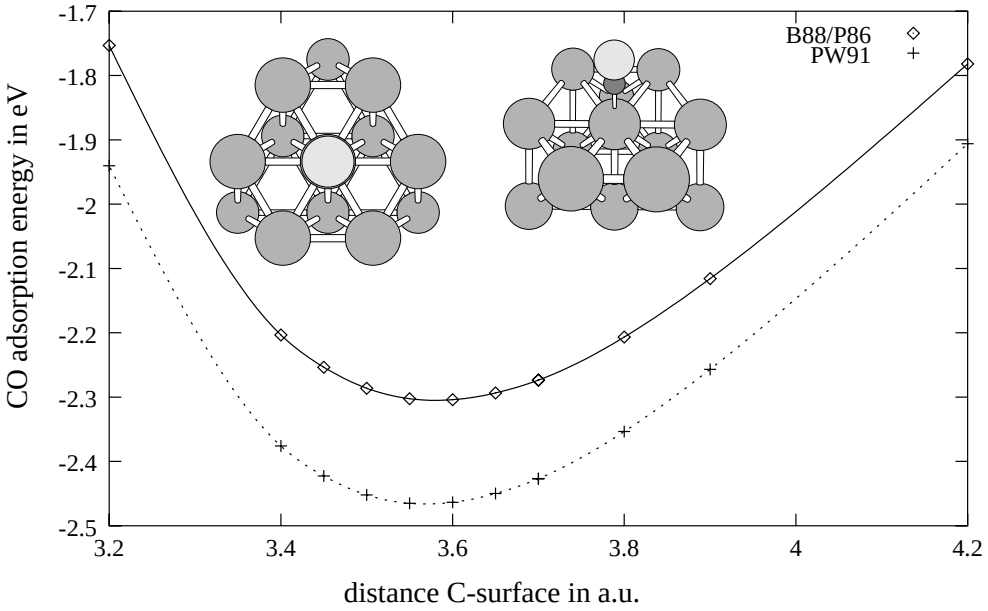

FIG. 1:

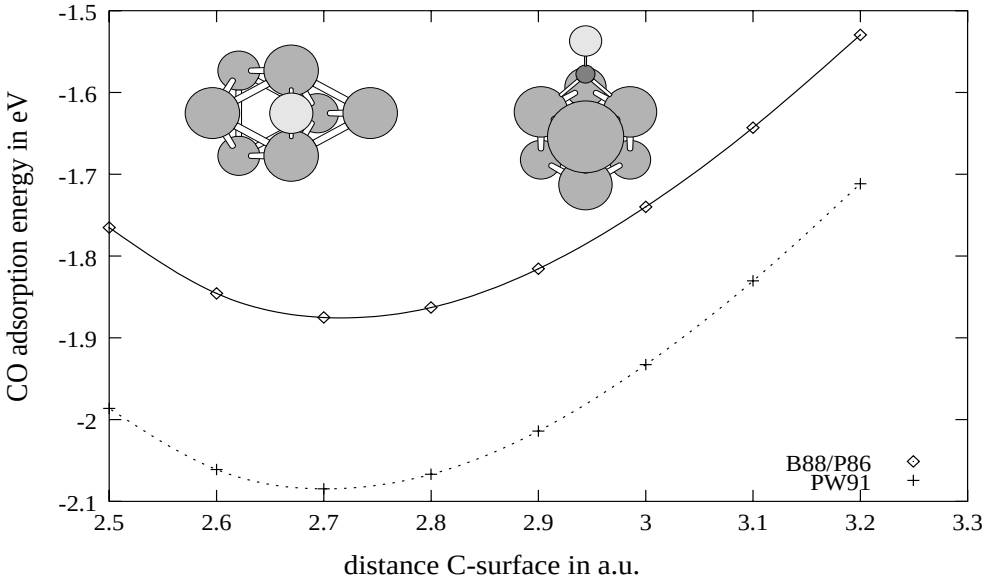
CO adsorption energy in eV
-1.5
-1.6
-1.7
-1.8
-1.9
-2
-2.1
2.5
2.6
2.7
2.8
2.9
3
3.1
3.2
3.3
distance C-surface in a.u.
B88/P86
PW91

FIG. 2:

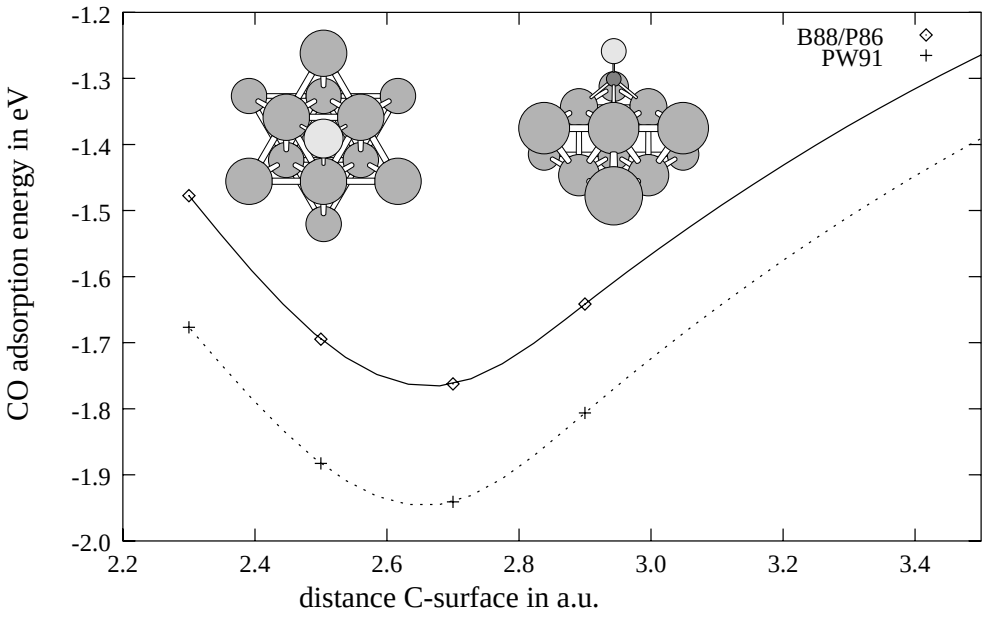
CO adsorption energy in eV
-1.2
-1.3
-1.4
-1.5
-1.6
-1.7
-1.8
-1.9
-2.0
2.2
2.4
2.6
2.8
3.0
3.2
3.4
distance C-surface in a.u.
B88/P86
PW91

FIG. 3:

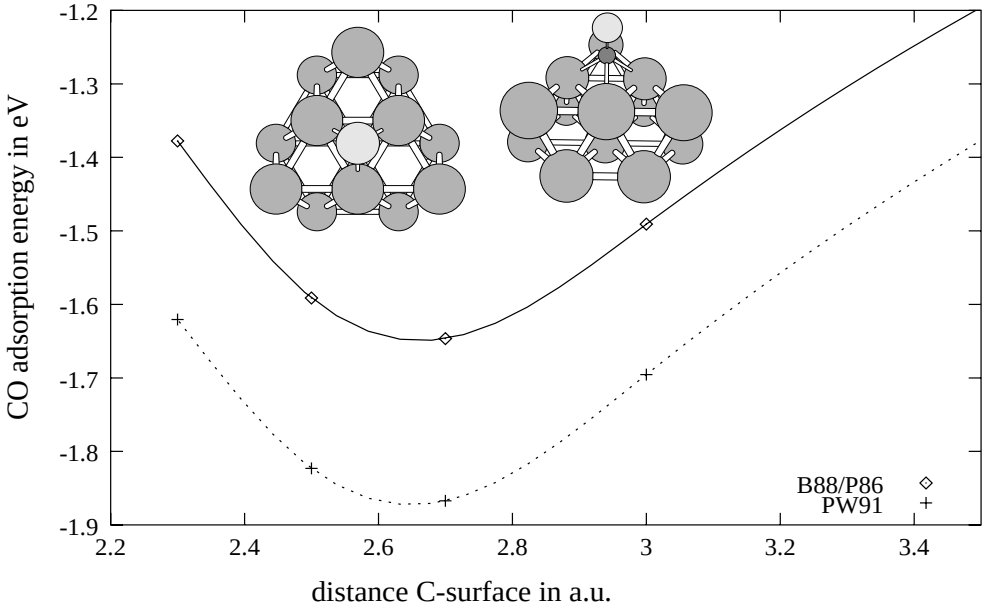
-1.2
-1.3
-1.4
-1.5
-1.6
-1.7
-1.8
-1.9
CO adsorption energy in eV
2.2
2.4
2.6
2.8
3
3.2
3.4
distance C-surface in a.u.
B88/P86
PW91

FIG. 4: